

See discussions, stats, and author profiles for this publication at: <https://www.researchgate.net/publication/273443103>

Synthesis, characterization and anticancer activity of gold(I) complexes that contain tri-tert-butylphosphine and dialkyl dithiocarbamate ligands

ARTICLE *in* EUROPEAN JOURNAL OF MEDICINAL CHEMISTRY · MARCH 2015

Impact Factor: 3.45 · DOI: 10.1016/j.ejmech.2015.03.019

CITATIONS

2

READS

93

10 AUTHORS, INCLUDING:



Mohamed Wazeer

King Fahd University of Petroleum and Miner...

134 PUBLICATIONS 1,157 CITATIONS

SEE PROFILE



Vikram Dhuna

DAV College Amritsar

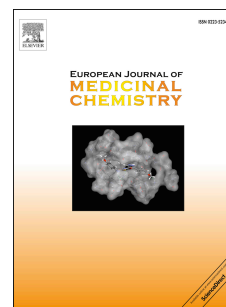
32 PUBLICATIONS 210 CITATIONS

SEE PROFILE

Accepted Manuscript

Synthesis, characterization and anticancer activity of gold(I) complexes that contain tri-*tert*-butylphosphine and dialkyl dithiocarbamate ligands

Muhammad Altaf, M. Monim-ul-Mehboob, Adam A.A. Seliman, Manzar Sohail, Mohammed I.M. Wazeer, Anvarhusein A. Isab, L. Li, V. Dhuna, G. Bhatia, K. Dhuna



PII: S0223-5234(15)00186-5

DOI: [10.1016/j.ejmech.2015.03.019](https://doi.org/10.1016/j.ejmech.2015.03.019)

Reference: EJMECH 7764

To appear in: *European Journal of Medicinal Chemistry*

Received Date: 11 November 2014

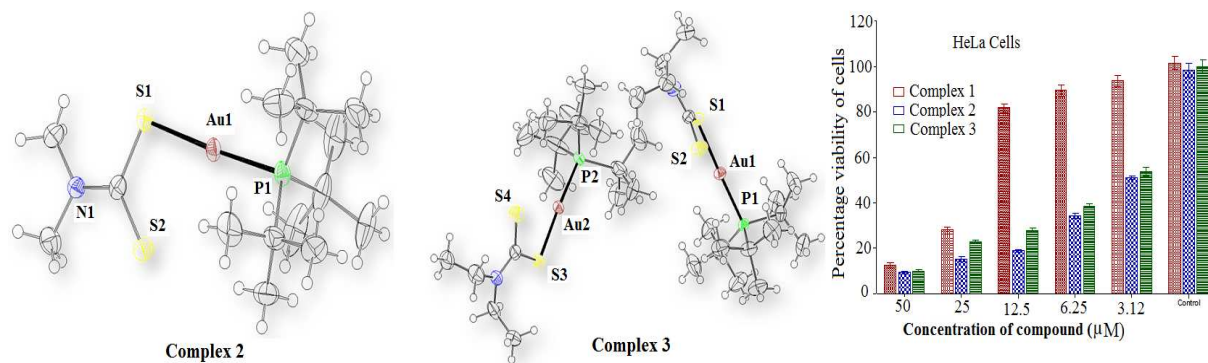
Revised Date: 8 March 2015

Accepted Date: 9 March 2015

Please cite this article as: M. Altaf, M. Monim-ul-Mehboob, A.A.A. Seliman, M. Sohail, M.I.M. Wazeer, A.A. Isab, L. Li, V. Dhuna, G. Bhatia, K. Dhuna, Synthesis, characterization and anticancer activity of gold(I) complexes that contain tri-*tert*-butylphosphine and dialkyl dithiocarbamate ligands, *European Journal of Medicinal Chemistry* (2015), doi: 10.1016/j.ejmech.2015.03.019.

This is a PDF file of an unedited manuscript that has been accepted for publication. As a service to our customers we are providing this early version of the manuscript. The manuscript will undergo copyediting, typesetting, and review of the resulting proof before it is published in its final form. Please note that during the production process errors may be discovered which could affect the content, and all legal disclaimers that apply to the journal pertain.

Two new linear gold(I) complexes of formulae $[\text{Au}\{\text{P}(\text{t-Bu})_3\}(\text{S}_2\text{CN}(\text{CH}_3)_2)]$ (**2**), and $[\text{Au}\{\text{P}(\text{t-Bu})_3\}(\text{S}_2\text{CN}(\text{C}_2\text{H}_5)_2)]$ (**3**) have been prepared. The structure of these complexes have been determined by single X-ray crystallography.



Synthesis, characterization and anticancer activity of gold(I) complexes that contain tri-*tert*-butylphosphine and dialkyl dithiocarbamate ligands

Muhammad Altaf^b, M. Monim-ul-Mehboob^a, Adam A. A. Seliman^a, Manzar Sohail^b,
Mohammed I. M. Wazeer^a, Anvarhusein A. Isab^{*a}, L. Li^c, V. Dhuna^d, G. Bhatia^c, K. Dhuna^e

^aDepartment of Chemistry, King Fahd University of Petroleum and Minerals, Dhahran 31261, Saudi Arabia

^bCenter of Excellence in Nanotechnology, King Fahd University of Petroleum and Minerals, Dhahran 31261, Saudi Arabia

^cKing Abdullah University of Science and Technology (KAUST), Thuwal 23955-6900, Jeddah, Saudi Arabia

^dDept. of Molecular Biology and Biochemistry, Guru Nanak Dev University, Amritsar-143005, Punjab, India

^eDepartment of Molecular Biology and Biochemistry, Guru Nanak Dev University, Amritsar – 143005, Punjab, India

Abstract

Two new gold(I) complexes that contain tri-*tert*-butylphosphine and dialkyl dithiocarbamate ligands were synthesized and characterized by FTIR, NMR spectroscopy, Cyclic voltammetry, elemental analysis and X-ray diffraction. The *in vitro* cytotoxicity of both complexes was examined against A549 (lung cancer), MCF7 (breast cancer), and HeLa (cervical cancer) human cancer cell lines. Both complexes exhibit very strong *in vitro* cytotoxic effects against A549, MCF7 and HeLa cell lines. The screening of the cytotoxic activity based on IC₅₀ data against the A549, MCF7, and HeLa lines shows that the synthesized gold(I) complexes are highly effective, particularly against HeLa cancer cell line. Based on IC₅₀ data, the cytotoxic activity of both complexes is better than well-known commercial anticancer drug cisplatin against all the three cancer lines tested.

Key words: Gold(I) complexes, Anticancer activity, Human A549, MCF7 and HeLa cell lines

32 Corresponding author Dr. A. A. Isab (aisab@kfupm.edu.sa)

1. Introduction

Cisplatin, carboplatin and oxaliplatin are widely used commercial platinum(II) based metallo-drugs which have been used effectively for the treatment of cancers [1-3]. However, the gamut of activity against different kinds of cancers is limited for such drugs [4]. The efficacy of platinum(II) anticancer drugs is mainly hampered due to some side effects such as neurotoxicity, ototoxicity, anemia, nausea [5] and the acquired as well as intrinsic resistances exhibited by cancer cell lines [6]. Such negative and limiting factors of platinum(II) drugs are major impediments in their clinical use invariably against all kind of cancers [7]. Therefore, non-platinum metals like gold compounds have been synthesized and evaluated for their potential augmented anticancer activity with much lower toxicity and fewer side effects against a wide panel of cancer cell lines.

Generally, the study of gold complexes, bearing different functional ligands exhibiting interesting physical, chemical, biological and pharmacological properties, has gained much attention [8-11]. Particularly, there was substantial interest in the coordination chemistry of Au(I) complexes showing biological activity with potential medicinal applications. For instance, the currently used drugs like *Auranofin*, *Solganol* and *Myocrisin* are Au(I)-S complexes [12-16]. Consequently, the gold(I) complexes have long been studied as anti-arthritis and anti-microbial agents [17-21]. It has been found that gold(I)-phosphine complexes with P-Au-P, P-Au-N, P-Au-S, and S-Au-S bonding show marked biological activities against bacteria and yeast [22-23]. The gold(I) phosphine complexes are known to exhibit promising anticancer properties [17, 24-26].

In this connection, Lorber *et al.* firstly reported in 1979 that *Auranofin* could inhibit the *in vitro* proliferation of HeLa cells [27]. McKeage and coworkers reported, bis(diphosphino)gold(I) compounds demonstrate prospective *in vivo* anticancer activities [28]. Berners-Price *et al.*

pointed out $[\text{Au}(\text{dppe})_2]^+$ and its derivatives as their credible *in vitro* and *in vivo* anticancer activities *via* the mitochondrial-mediated apoptotic pathway [29]. V. Gandin *et al.* reported that phosphine gold(I) complexes efficiently inhibited cytosolic and mitochondrial (TrxR) [30]. Ott *et al.* reported gold(I) phosphine complex containing a naphthalimide ligand behaves as a TrxR inhibiting antiproliferative agent and angiogenesis inhibitor [31]. Che *et al.* described anticancer gold(I)–phosphine complexes as potent autophagy-inducing agents [32].

In the last decade, a new class of gold complexes with dithiocarbamate ligands has been emerged as potential anticancer agents. In this regards, Fregona and coworkers firstly prepared and characterized some novel gold(III) dithiocarbamate compounds containing N,N-dimethyldithiocarbamate and ethylsarcosinedithiocarbamate exhibiting the promising chemical and biological profile [33]. Similarly, significant inhibitory effect of dibromo(N,N-dimethyldithiocarbamato)gold(III) *in vivo* was reported against growth of MDA-MB-231 breast tumor cells (BTC) [34]. Gold(I)-dithiocarbamate species, could inhibit the chymotrypsin-like activity of purified 20S proteasome and 26S proteasome in human breast cancer MDA-MB-231 cells [35].

Gold(I) thiolates employed clinically in the treatment of rheumatoid arthritis displayed some potency against various tumors but a greater potential is found in their analogues. In particular, analogues featuring a linear P-Au-S arrangement in which the thiolate ligand is derived from a biologically active thiol display high potency [36]. Recently, F.K. Keter *et al.* synthesized new gold(I) complexes containing PPh_3 =triphenylphosphine or dppp = 1,3-bis(diphenylphosphino)propane or dpph = 1,6-bis-(diphenylphosphino)hexane and L = pyrazolyldithiocarbamate or 3,5-dimethylpyrazolyldithiocarbamate or indazolyldithiocarbamate and found all complexes active against human cervix epithelioid carcinoma (HeLa) cells [37].

Here, we are reporting the synthesis of gold(I) complexes of tertiarybutylphosphine with dialkyldithiocarbamate as co-ligands, their structure determination by single crystal X-ray crystallography and their structural analysis by FTIR and NMR measurements. Finally, the well characterized gold(I) complexes have been subjected to *in vitro* cytotoxic evaluation against three standard human cancer cell lines named, A549, MCF7, and HeLa cell lines.

2. Materials and physical methods

Sodium dimethyldithiocarbamate monohydrate, sodium diethyldithiocarbamate trihydrate were purchased from Sigma-Aldrich Co. St. Louis, Missouri United States. Chloro(tri-tert-butylphosphine)gold(I) (**1**) as gold(I) precursor was obtained from Strem Chemicals, Inc., Newburyport, Massachusetts, United States. All solvents including ethanol, dichloromethane were purchased from Merck Darmstadt, Germany and used without further purification. All reactions were carried out under normal ambient conditions. Human lung cancer and human breast cancer, human cervical cancer cell lines were procured from National Centre for Cell Sciences (NCCS), Pune, India.

Elemental analyses of (dialkyldithiocarbamate)(tert-butylphosphine)gold(I) complexes (**2** and **3**) were performed on Perkin Elmer Series 11 (CHNS/O), Analyzer 2400. The solid state FTIR spectra of free ligands and their corresponding gold(I) complexes were recorded on a Perkin-Elmer FTIR 180 spectrophotometer or NICOLET 6700 FTIR using Potassium bromide (KBr) pellets over the range 4000–400 cm^{-1} and Far-IR spectra were recorded for gold complexes at 4 cm^{-1} resolution at room temperature using Cesium chloride (CsCl) disks on a Nicolet 6700 FTIR with Far-IR beam splitter. The IR frequencies (cm^{-1}) of free ligands and Au(I) complexes are given in Table 1.

^1H , ^{13}C , and ^{31}P NMR spectra were recorded on a LAMBDA 500 spectrophotometer operating at 500.01, 125.65 and 200.0 MHz respectively, corresponding to a magnetic field of 11.74 T. Tetramethylsilane (TMS) was used as an internal standard for ^1H and ^{13}C , while Triphenylphosphine (TPP) was used as an external standard for ^{31}P NMR spectra. The ^{13}C NMR spectra were obtained with ^1H broadband decoupling, and the spectral conditions were: 32 k data points, 0.967 s acquisition time, 1.00 s pulse delay and 45 pulse angle. The ^1H , ^{13}C and ^{31}P NMR chemical shifts are given in Tables 2-3, respectively.

3. Results and Discussion

3.1. FTIR Characterization

Dithiocarbamate compounds can be identified *via* the presence of certain absorbance peaks primarily vibrational $\nu(\text{C-N})$ and $\nu(\text{C-S})$. In the infrared spectra of dithiocarbamate compounds, the region $1480\text{--}1550\text{ cm}^{-1}$ is primarily associated with the $\text{R}_2\text{N-CS}_2$ 'thioureide' band which defines the carbon-nitrogen bond order between a single bond at $1250\text{--}1350\text{ cm}^{-1}$ and a double bond at $1640\text{--}1690\text{ cm}^{-1}$ [38].

In the IR spectra, the most important thioureide band, $\nu(\text{C-N})$ was observed at 1479 and 1478 cm^{-1} for complexes (2) and (3) respectively. Since these frequency modes lie in between those associated with single C-N and double C=N bonds hence the partial double bond character of thioureide bond was confirmed for both of the complexes [39]. The presence of thioureide band between $1430\text{--}1545\text{ cm}^{-1}$ suggests a considerable double bond character in the C-N bond vibration of the $\text{R}_2\text{N-CS}_2$ group [40]. This strong absorption band ($1480\text{--}1542\text{ cm}^{-1}$) is known as the thioureide ion band. The band appears intermediate within C-N single bond (C-N: $1063\text{--}1261\text{ cm}^{-1}$) and double bond (C=N: $1640\text{--}1690\text{ cm}^{-1}$). This band shows the partial double bond characteristic of dithiocarbamate ($\text{S}_2\text{C-NR}_2$). Such partial double bond culminates into stretching

vibration due to the partial delocalization of electron density within the dithiocarbamate moiety [41]. A strong absorption band in the range of 1480-1542 cm^{-1} gives additional confirmation of the gold(I) complexes formation [42].

The C=S thiocarbonyl stretch splits into two peaks (doublet) at 1022, 972 cm^{-1} and 1020, 989 cm^{-1} with medium intensity in the spectra of complexes **(2)** and **(3)** respectively. The bands present in the range of 972-1022 cm^{-1} is attributed to the customary contribution of (C...S). The splitting of $\nu(\text{C-S})$ bands in the range 965-972 cm^{-1} indicates a monodentate nature of dialkyl dithiocarbamate ligands in the synthesized complexes [43-45]. In addition to the polar thioureide ion band, the usual bands for sp^3 -hybridized carbon-hydrogen stretches are observed in the range of 2840-3000 cm^{-1} [46]

The stretching band frequencies are observed for the saturated aliphatic C-H methyl group of coordinated dialkyl (methyl/ethyl) dithiocarbamate at 2962(asym), 2869(sym) and 2965(asym), 2867(sym) cm^{-1} for complexes **(2)** and **(3)** respectively. The C-H ($-\text{CH}_3$) methyl groups have characteristic bending absorptions at 1372 and 1371 cm^{-1} in the spectra of complexes **(2)** and **(3)** respectively. The C-H bending band(s) associated C-H stretching band(s) are often determining factor of methyl groups in a molecule. The C-H ($-\text{CH}_2-$) methylene coordinated diethyldithiocarbamate stretching occurs at 2925 cm^{-1} and its corresponding bending appears at 1409 cm^{-1} for complex **(3)** [47-48].

The band at 304 cm^{-1} in the far-IR spectrum of complex **(1)** has been assigned to the $\nu(\text{Au-Cl})$ vibration, while bands appearing at 282 and 194 cm^{-1} are attributed to $\nu(\text{Au-S})$ and $\nu(\text{Au-P})$ vibrations for complexes **(2)** and **(3)** respectively [49-53].

3.2. NMR Characterization

The ^1H NMR chemical shifts of gold(I) complexes (**1-3**) and free dialkyl dithiocarbamate ligands are listed in Table 2. A small upfield shift for methyl protons of tri-*ter*-butyl group was observed for complex (**2**) compared to complex (**1**). Whereas, a small downfield shift for methyl protons of tri-*ter*-butyl group have been observed for complex (**3**) as shown in Table 2. The small upfield shifts for proton(s) of the coordinated dimethyldithiocarbamate and diethyldithiocarbamate have been observed in gold(I) complexes (**2** and **3**) in comparison to free dialkyl dithiocarbamate ligands.

The ^{13}C and ^{31}P NMR chemical shifts of complexes (**2**) and (**3**) along with their corresponding gold(I) precursor (**1**) and free dialkyldithiocarbamate ligands are tabulated in Table 3. In the ^{13}C NMR spectra four and five resonances are observed for complexes (**2**) and (**3**) respectively. Small shielding in the chemical shifts was observed for methyl carbons and quaternary carbon bonded to phosphorus in tri-*ter*-butylphosphine in the complexes (**2** and **3**) as compare to gold(I) precursor. There are also small upfield chemical shifts for CH_3 , CH_2 and $\text{C}=\text{S}$ carbons of coordinated dialkyldithiocarbamate with respect to free dialkyl dithiocarbamate ligands. The ^{13}C chemical shifts of $\text{C}=\text{S}$ carbon of free dimethylthiocarbamate and diethylthiocarbamate ligands are observed in the range 205-212 ppm. The upfield shifts are observed for coordinated dialkyldithiocarbamates in complexes (**2**) and (**3**). The P-C coupling constant ($J_{\text{p-c}}$) showed a reduction of 3 Hz on complexation.

3.3. Crystal structure of complex (**2**)

The molecular structure of complex (**2**) is shown in Figure 1. X-ray structure contains one molecule of complex $[\text{t-Bu}_3\text{PAu}(\text{S}_2\text{CNMe}_2)]$ (**2**) in crystallographic asymmetric unit. The monodentate mode of coordination of the dithiocarbamate ligand is reflected in the difference of

C–S bond lengths with the shortest of these being associated with the weakly bonded S2 atom as shown in Table 4. The gold(I) atom is coordinated with P and S atoms of tri-*ter*-butylphosphine and dimethyl dithiocarbamate ligands respectively. The Au1–S1 and Au1–P1 bond distances are 2.3247 (15) and 2.2743 (14) Å respectively. The P1–Au1–S1 bond angle is 176.44 (4)°, which shows Au(I) atom adopts distorted linear geometry. The Au–S bond length is longer than Au–P bond length. The deviation from the ideal linear geometry around gold can be attributed to the presence of a close intra-molecular Au1...S2 contact of 3.127 Å. The Au–S and Au–P bond lengths are similar to those found in [Et₃PAu(S₂CNEt₂)] complex [54]. However, the S–Au–P bond angle is different from [Et₃PAu(S₂CNEt₂)] complex [54] and other [t-Bu₃PAu]⁺ complexes [55-58].

3.4. Crystal structure of complex (3)

X-ray structure of complex (3) is shown in Figure 2. There are two independent molecules of gold(I) complex in the asymmetric unit cell. In both molecules, gold(I) atom is coordinated with one P donor atom of tri-*ter*-butylphosphine ligand and S atom of diethyl dithiocarbamate ligand. There are only minor conformational differences between x-ray structure of two molecules. The Au1–S1 and Au2–S3 bond distances are 2.3293 (15) and 2.3139 (16) Å respectively. The Au1–P1 and Au–P2 bond distances are 2.2818 (15) and 2.2753 (16) Å. The Au–S bond distances are very much similar to [t-Bu₃PAu(S₂CNMe₂)] (2) and [Et₃PAu(S₂CNEt₂)] complexes [54]. The Au–P bond distances are different than [Et₃PAu(S₂CNEt₂)] complex [54] and similar to [t-Bu₃PAu(S₂CNMe₂)] (2) complex. The geometry around Au1 and Au2 atoms is conventionally distorted linear and similar to [t-Bu₃PAu(S₂CNMe₂)] (2) and [Et₃PAu(S₂CNEt₂)] complexes [60]. In molecules 1 and 2, S1–Au1–P1 and S3–Au2–P2 bond angles are 172.74 (6) and 170.42 (6)° respectively. More distortion

from ideal linear geometry is observed in each molecule of complex (3) than complex (2). It is interesting to correlate the magnitude of the intra-molecular Au-S interactions with the deviations from linearity of the P-Au-S bond. In complex (3), where the Au1...S2 and Au2...S4 interactions are longer, the deviation from the ideal linear angle of 180° is increased. The bond angle values around central Au(I) atom in molecule 1 and 2 confirm the presence of pseudo linear geometry in complex (3). The overall geometry of [t-Bu₃PAu(S₂CNEt₂)] (3) closely resembles to those Au(I) complexes that contain [t-Bu₃PAu]⁺ unit [55-58].

3.5. Electrochemical study of gold(I) complexes (1-3)

Cyclic Voltammetry of complexes (1, 2 and 3) is given in Figure 3. Quasireversible redox couple corresponding to [Au(t-BuP)Cl]⁰ / [Au(t-BuP)Cl]²⁺ appears at 1.19 V while for complexes (2 and 3) this redox couple appears at 1.24 V and 1.41 V, respectively. Higher potentials for redox couples of complexes (2 and 3) are indicative of the difficulty in gold(I) oxidation due to stabilizing effect of the dialkyldithiocarbamate ligands [59]. Increase in chain length with corresponding increase in electron donating effect of alkyl groups of the ligands is responsible for a higher anodic potential of complex (3) compared to complex (2). Thus, higher oxidation potentials of Au(I) in complexes (2 and 3) are indicative of their higher stability compared to complex (1) under physiological conditions. All three complexes show one reduction process, which is attributed to the gold(I) – gold(0) reduction. For complex (1) reduction peak appears at 0.167 V while for complex (3); it is at 0.0848 V and for complex (2) at -0.019 V.

3.6. *in vitro* anticancer activities of complexes (1-3)

Modern oncologic or anticancer studies aim towards finding newer compounds with less cytotoxic potential than cisplatin toxicity. In this connection, gold(I) complexes with various

ligands including Au–N, Au–S or Au–C bonds are being extensively developed and investigated for their bioactivities as cytotoxic agents [60]. In this study, new gold(I) complexes (**2** and **3**) are developed by replacing one chlorido ligand in gold(I) precursor complex (**1**) with dialkyldithiocarbamate ligand. The synthesized complexes (**2** and **3**) are subjected to *in vitro* cytotoxic evaluation against A549, MCF7 and HeLa cancer cell lines using MMT assay.

The dose dependent cytotoxic effect was obtained by the stipulated increase in concentrations of complexes (**1**), (**2**) and (**3**) against the fixed number of human cancer cells as shown in Figure 4-6. The IC_{50} concentration of complexes (**1**), (**2**) and (**3**) for different human cell lines are obtained from a curve between complex concentration and percentage viability of cells as shown in Figures S1-S3. The IC_{50} values of all complexes are in the range of 2.11 ± 0.43 to $26.90 \pm 1.04 \mu M$ as given in Table 4.

The *in vitro* cytotoxicity in terms of IC_{50} values against A549 cell line were found 41.60 ± 3.00 , 14.30 ± 0.81 , 26.90 ± 1.04 and $19.40 \pm 0.64 \mu M$ for cisplatin and gold(I) complexes (**1**), (**2**) and (**3**) respectively. The precursor complex (**1**) and synthesized complexes (**2** and **3**) have shown cytotoxicity almost two-three folds better than cisplatin. In MCF7 cancer cell line, *in vitro* anticancer activity in terms of IC_{50} values were 22.38 ± 0.62 , 16.71 ± 0.80 , 21.07 ± 0.95 and $16.00 \pm 0.83 \mu M$ for cisplatin and gold(I) complexes (**1**), (**2**) and (**3**) respectively. The precursor complex (**1**) and synthesized complexes (**2** and **3**) have anticancer activity close to cisplatin. For HeLa cancer cell line, *in vitro* cytotoxicity in terms of IC_{50} values were 19.40 ± 1.85 , 16.03 ± 1.01 , 2.11 ± 0.43 and $3.18 \pm 0.54 \mu M$ for cisplatin and gold(I) complexes (**1**), (**2**) and (**3**) respectively. Against HeLa cell line cytotoxicity of gold(I) complexes (**2** and **3**) is six to eight times better than cisplatin and gold(I) precursor complex (**1**). Newly synthesized complexes (**2**) and (**3**) were found to be most effective against HeLa cell line in terms of IC_{50} values. Against

HeLa cell line cytotoxicity of complexes (**2** and **3**) is better than the equivalent $\text{Au}(\text{PEt}_3)\text{Cl}$, as the following IC_{50} (μM) value against the same line show: $\text{Au}(\text{PEt}_3)\text{Cl}$: 1.7(0.06) μM [61].

The better inhibition of growth of cancer cells by synthesized complexes (**2** and **3**) than gold(I) precursor complex (**1**) can be attributed to dithiocarbamate as labile co-ligands bonded with central gold(I) ions. Overall, the anticancer activity of synthesized complexes (**2** and **3**) against, A549, MCF7 and HeLa human cancer cell lines is interesting and better activity than previous anticancer studies of gold compounds [62-65].

4. Conclusions

In this report, cytotoxic activity of two gold(I) complexes with S–Au–P fragment against A549, MCF7 and HeLa human cancer cell lines have been evaluated and these complexes exhibit very strong cytotoxic effects *in vitro*. The new complexes (**2** and **3**) with the dimethyldithiocarbamate and diethyldithiocarbamate ligands showed excellent cytotoxic activity against HeLa human cancer cell line. These results show good inhibition and selectivity of both complexes against HeLa cell line which is very important in drug design inhibition of target biomolecules. In short, the IC_{50} data reveals that complexes (**2** and **3**) are much better cytotoxic agents than commonly used cisplatin. The significant cytotoxic activity of gold(I) complexes (**2** and **3**) has made them strong candidates as potential anticancer agents for further exploration against cervical cancer.

5. Experimental

5.1. Synthesis of $[\text{t-Bu}_3\text{PAu}(\text{S}_2\text{CNMe}_2)]$ (**2**)

Sodium dimethyldithiocarbamate monohydrate (0.072 g, 0.05 mmol) dissolved in 15 mL ethanol was added drop wise to [t-Bu₃PAuCl] (0.217 g, 0.05 mmol) contained in 10 mL dichloromethane at room temperature and solution was continuously stirred for 3h. The clear light yellow solution obtained was filtered to avoid any impurity and kept undisturbed at room temperature for crystallization by slow evaporation. After seven days colorless block like crystals were obtained. A suitable quality crystal was chosen for X-ray diffraction analysis. Anal. Calc. for C₁₅H₃₃AuNPS₂: C, 34.68; H, 6.40; N, 2.70; S, 12.34; Found: C, 34.80; H, 6.33; N, 2.82; S, 12.43. Yield: 0.242 g, (93%).

5.2. Synthesis of [t-Bu₃PAu(S₂CNEt₂)] (3)

Sodium diethyldithiocarbamate trihydrate (0.113 g, 0.05 mmol) dissolved in 15 mL of ethanol was added dropwise to [t-Bu₃PAuCl] (0.217 g, 0.05 mmol) contained in 10 mL dichloromethane at room temperature with continuous stirring for 3h. The transparent yellow solution obtained was filtered to avoid any impurity and kept undisturbed for slow evaporation at room temperature. After five days colorless block like crystals were obtained. A suitable quality crystal was chosen for X-ray diffraction analysis. Anal. Calc. for C₁₇H₃₇AuNPS₂: C, 37.29; H, 6.81; N, 2.56; S, 11.71; Found: C, 37.19; H, 6.37; N, 2.70; S, 11.68. Yield: 0.260 g, (95%).

5.3. Stability of gold(I) complexes in DMSO-d₆

¹H and NMR spectra of complexes (2 and 3) in DMSO-d₆ solvent were measured for their stability test. The extent of decomposition over time was determined by comparing the NMR spectra collected after 1, 6, 12, 24, 48 and 72 h. No significant change in the chemical shifts and

the splitting patterns of complexes (**2** and **3**) were observed in their time dependent ^1H and ^{13}C NMR spectra.

5.4. X-ray structure determination

For both gold(I) complexes (**2**) and (**3**), good quality single crystal was chosen and mounted on a plastic loop to an Agilent Super Nova diffractometer equipped with a Mo-K α radiation ($\lambda = 0.71073 \text{ \AA}$). The data were collected and integrated with CrysAlisPRO [66]. The refinement and all further calculations were carried out using SHELXL [67]. The H-atoms were either located from Fourier difference maps and freely refined or included in calculated positions and treated as riding atoms using SHELXL default parameters. The non-H atoms were refined anisotropically, using weighted full-matrix least-squares on F^2 . Empirical or multiscan absorption corrections were applied using the SCALE3 ABSPACK [68]. Graphics were generated using PLATON [69]. A summary of crystal data and refinement details for gold(I) complexes (**2**) and (**3**) are given in Table 5. Selected bond lengths and bond angles are given in Table 6.

5.5. Electrochemistry

Electrochemical measurements were undertaken on an Autolab PGSTAT-128N (Eco-Chemie) workstation. A standard three electrode electrochemical cell utilizing a membrane Pt-disc working electrode, a double junction Ag/AgCl/3M KCl reference electrode and platinum wire auxiliary electrode was used in all voltammetric experiments. 10 mM of all compounds were dissolved in acetonitrile containing 100 mM of Potassium thiocyanate as an electrolyte.

5.6. MTT assay for *in vitro* anticancer of complexes (1-3)

A549, MCF7 and HeLa human cancer cells were seeded and maintained on Dulbecco's Modified Eagle's Medium (DMEM) supplemented with streptomycin (100 U/mL), gentamycin (100 µg/mL), 10% FBS (Fetal Bovine Serum) at 37 °C and humid environment containing 5% CO₂. MTT was used to assess cell integrity and *in vitro* anticancer. The uptake of the vital mitochondrial dye, 3-[4,5-dimethylthiazol-2-yl]- 2,5-diphenyl tetrazolium bromide (MTT) was monitored by cell mitochondria [70]. The cells were grown in 96 well flat bottom tissue culture plates at a concentration of 5×10^3 cells / well in DMEM medium. After 72 h of growth, three cancer cell lines, A549, MCF7 and HeLa and were treated with gold(1) complexes (**1-3**) and cisplatin at concentration from 3.12 to 50 µM. After 24 h, 100 µL of MTT was added to each well and incubated the plate for 4 h at 37°C in dark. The treated plate was then removed and 100 µL of DMSO (Dimethylsulfoxide) was added in each well. Mixture in each well was subjected to mixing well by repeated pipetting in and out to bring out the formazan. The absorbance was read out at 570 nm in ELISA (Enzyme-linked immunosorbent assay) reader. The cell viability values were expressed as the mean \pm standard error of the mean (SEM) from at least three independent experiments. The IC₅₀ concentrations of gold(1) complexes (**1-3**) used were calculated from a separate curve between complex concentration and average % viability of cells plotted in Microsoft Excel 2007 (graphs not shown) using MTT assay data and explained by logarithmic regression equations (equations not shown).

Supplementary material

Supplementary crystallographic data of CCDC deposit number is 946806 and 946805 for the complexes (**2** and **3**) respectively and can be obtained free of charge via

www.ccdc.cam.ac.uk/data_request/cif, by e-mailing data_request@ccdc.cam.ac.uk, or by contacting the Cambridge Crystallographic Data Centre, 12 Union Road, Cambridge CB2 1EZ, UK; fax: +44(0)1223-336033.

Acknowledgement

The author(s) would like to acknowledge the support provided by King Abdulaziz City for Science and Technology (KACST) through the Science & Technology Unit at King Fahd University of Petroleum & Minerals (KFUPM) for funding this work through project No. *14-MED64-04* as part of the National Science, Technology and Innovation Plan.

References

- [1] B. Rosenberg, L. Van Camp, T. Krigas, *Nature*. 205 (1965) 698–699.
- [2] Y. Kidani, M. Noji, T. Tashiro, *Gann*. 71 (1980) 637–643.
- [3] N.J. Wheate, S. Walker, G.E. Craig, R. Oun, *Dalton Trans.* 39 (2010) 8113–8127.
- [4] E. Wong, C.M. Giandomenico, *Chem Rev.* 99 (1999) 2451–2466.
- [5] V.G. Schweitzer, *Otolaryngol Clin. North Am.* 26 (1993) 759–789.
- [6] D.J. Stewart, *Crit. Rev. Oncol. Hematol.* 63 (2007) 12–31.
- [7] S. Dhar, S.J. Lippard, Current Status and Mechanism of Action of Platinum-Based Anticancer Drugs, in *Bioinorganic Medicinal Chemistry* (ed E. Alessio), Wiley-VCH Verlag GmbH & Co. KGaA, Weinheim, Germany. (2011) 79–93.
- [8] K. Nomiya, R.S. Yamamoto, R. Noguchi, H. Yokoyama, N.C. Kasuga, K. Ohya, C. Kato, *J Inorg Biochem.* 95 (2003) 208–220.
- [9] T. McCormick, W.L. Jia, S. Wang, *Inorg Chem.* 45 (2006) 147–155.
- [10] S.S. Al-Jaroudi, M.I.M. Wazeer, A.A. Isab, S. Altuwaijri, *Polyhedron*. 50 (2013) 434–442.
- [11] R.B. Bostancioglu, K. Isik, H. Genc, K. Benkli, A.T. Koparal, *J Med Chem.* 27 (2012) 458–466.
- [12] S.H. van Rijt, P.J. Sadler, *Drug Discovery Today*. 14 (2009) 1089–1097.
- [13] R. Noguchi, A. Hara, A. Sugie, K. Nomiya, *Inorg Chem Commun.* 9 (2006) 355–359.
- [14] K. Nomiya, R. Noguchi, K. Ohsawa, K. Tsuda, M. Oda, *J Inorg Biochem.* 78 (2000) 363–370.

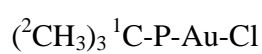
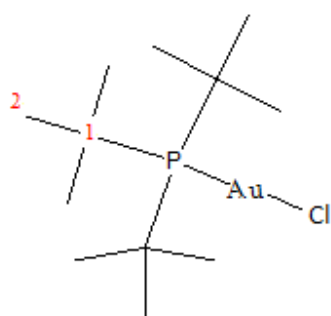
- [15] B.P. Howe, *Metal-Based Drugs*. 4 (1997) 273–277.
- [16] C. Frank Shaw III, *Chem Rev.* 99 (1999) 2589–2600.
- [17] O. Crespo, V.V. Brusko, M.C. Gimeno, M.L. Tornil, A. Laguna, N.G. Zabiroy, *Eur J Inorg Chem.* 2 (2004) 423–430.
- [18] K. Nomiya, R. Noguchi, M. Oda, *Inorg Chim Acta.* 298 (2000) 24–32.
- [19] H. Q. Liu, T.-C. Cheung, S.-M. Peng, C.-M. Che, *J Chem Soc Chem Commun.* (1995) 1787–1788.
- [20] C.J. O'Connor, E. Sinn, *Inorg Chem.* 17 (1978) 2067–2071.
- [21] M.A. Cinellu, G. Minghetti, M.V. Pinna, S. Stoccoro, A. Zucca, M. Manassero, M. Sansoni, *J Chem Soc Dalton Trans.* (1998) 1735–1742.
- [22] K. Nomiya, S. Takahashi, R. Noguchi, *J Chem Soc Dalton Trans.* (2000) 2091–2097.
- [23] R.C. Elder, K. Ludwig, J.N. Cooper, M.K. Eidsness, *J Am Chem Soc.* 107 (1985) 5024–5025.
- [24] R.W.-Y. Sun, C.-M. Che, *Coord Chem Rev.* 253 (2009) 1682–1691.
- [25] P. Papathanasiou, G. Salem, P. Waring, A.C. Willis, *J Chem Soc Dalton Trans.* (1997) 3435–3443.
- [26] H. Lv, B. Yang, J. Jing, Y. Yu, J. Zhang, J.-L. Zhang, *Dalton Trans.* 41 (2012) 3116–3118.
- [27] T.M. Simon, D.H. Kunishima, G.J. Vibert, A. Lorber, *Cancer.* 44 (1979) 1965–1975.
- [28] M J. McKeage, P. Papathanasiou, G. Salem, A. Sjaarda, G.F. Swiegers, P. Waring, S.B. Wild, *Metal-Based Drugs.* 5 (1998) 217–223.
- [29] S.J. Berners-Price, C.K. Mirabelli, R.K. Johnson, M.R. Mattern, F.L. McCabe, L.F. Faucette, C.M. Sung, S.M. Mong, P.J. Sadler, S.T. Crooke, *Cancer Res.* 46 (1986) 5486–5493.

- [30] V. Gandina, A.P. Fernandes, M.P. Rigobello, B. Dani, F. Sorrentino, F. Tisato, M. Björnstedt, A. Bindoli, A. Sturaro, R. Rella, C. Marzano, *Biochem Pharm.* 79 (2010) 90–101.
- [31] I. Ott, X. Qian, Y. Xu, D.H.W. Vlecken, I.J. Marques, D. Kubutat, J. Will, W.S. Sheldrick, P. Jesse, A. Prokop, C.P. Bagowski, *J Med Chem.* 52 (2009) 763–770.
- [32] S. Tian, F-M. Siu, S.C.F. Kui, C-N. Lok, C-M. Che, *Chem Commun.* 47 (2011) 9318–9320.
- [33] L. Ronconi, L. Giovagnini, C. Marzano, F. Bettio, R. Graziani, G. Pilloni, D. Fregona, *Inorg Chem.* 44 (2005) 1867–1881.
- [34] V. Milacic, D. Chen, L. Ronconi, K.R. Landis-Piwowar, D. Fregona, Q.P. Dou, *Cancer Res.* 66 (2006) 10478–10486.
- [35] X. Zhang, M. Frezza, V. Milacic, L. Ronconi, Y. Fan, C. Bi, D. Fregona, Q.P. Dou, *J Cell Biochem.* 109 (2010) 162–72.
- [36] E.R. Tiekink, *Crit Rev Oncol Hematol.* 42 (2002) 225–248.
- [37] F.K. Keter, I.A. Guzei, M. Nell, W.E. van Zyl, J. Darkwa, *Inorg Chem.* 53 (2014) 2058–2067.
- [38] A.J. Odola, J.A.O. Woods, *J Chem Pharm Res.* 3 (2011) 865–871.
- [39] F. Jian, Z. Wang, Z. Bai, X. You, H. Fun, K. Chinnakali, L.A. Razak, *Polyhedron.* 18 (1999) 3401–3406.
- [40] A. Jayaraju, M.M. Ahamad, R.M. Rao, J. Sreeramulu, *Der Pharma Chemica* 4 (2012) 1191–1194.
- [41] H. Nabipour, S. Ghammamy, S. Ashuri, Z.S. Aghbolagh, *J Org Chem.* 2 (2010) 75–80.
- [42] J. Chatt, L.A. Duncanson, L.M. Venanzi, *Nature.* 177 (1956) 1042–1043.

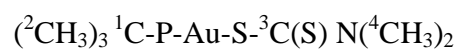
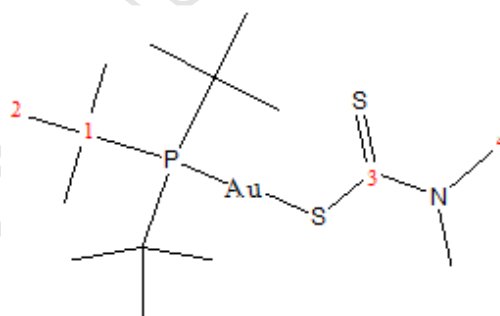
- [43] I. Raya, I. Baba, B.M. Yamin, Malaysia Journal of Analytical Sciences. 10 (2006) 93–98.
- [44] W. Haas, T. Schwarz, Microchem Ichonal Acta. 58 (1963) 253–259.
- [45] D.C. Onwudiwe, P.A. Ajibade, Polyhedron. 29 (2010) 1431–1436.
- [46] C.J. Pouchert, Aldrich Library of FT-IR Spectra. Second Ed.; Aldrich Chemical Company: Milwaukee. (1997).
- [47] D.L. Pavia, G.M. Lampman, S.G. Kriz, Introduction to Spectrochemistry. third ed., Thomson Learning, USA. (2001).
- [48] R.M. Silverstein, F.X. Webster, Spectrometric Identification of Organic Compounds. Sixth Ed., Wiley, New York. (1998).
- [49] T.W.G. Solomons, C. Fryhle, Study Guide to Organic Chemistry. Organic Chemistry, seventh Ed., Wiley, New York. (2000).
- [50] K.N. Kouroulis, S.K. Hadjikakou, N. Kourkouvelis, M. Kubicki, L. Male, M. Hursthouse, S. Skoulika, A.K. Metsios, V.Y. Tyurin, A.V. Dolganov, E.R. Milaevag, N. Hadjiliadis, Dalton Trans. (2009) 10446–10456.
- [51] E.A. Allen, W. Wilkinson, Spectrochim Acta. 28 (1972) 2257–2262.
- [52] I.S. Butler, A. Neppel, K.R. Plowman, C.F. Shaw, J Raman Spectrosc. 15 (1984) 310–318.
- [53] A.G. Jones, D.B. Powell, Spectrochim Acta. 40 (1984) 563–570.
- [54] S.Y. Ho, E.R.T. Tiekink, Z. Kristallogr. 220 (2005) 342–344.
- [55] I. Sanger, H.-W. Lerner, T. Sinke, M. Bolte, Acta Cryst. E68 (2012) m708.
- [56] P. Lu, T.C. Boorman, A.M.Z. Slawin, I. Larrosa, J. Am. Chem. Soc. 132 (2010) 5580–5581.
- [57] R.E. Marsh, Acta Cryst. B58 (2002) 893–899.

- 431 [58] M. Altaf, M. Monim-ul-Mehboob, A. A. Isab, V. Dhuna, G. Bhatia, K. Dhuna, S.
432 Altuwaijri, *New J. Chem.*, 39 (2015) 377-385.
- 433 [59] M. Serratrice, M. A. Cinellu, L. Maiore, M. Pilo, A. Zucca, C. Gabbiani, A. Guerri, I.
434 Landini, S. Nobili, E. Mini, L. Messori, *Inorg Chem*, 51 (2012) 3161–3171.
- 435 [60] I. Ott, R. Gust, *Arch Pharm Chem Life Sci.* 340 (2007) 117–126.
- 436 [61] E. Barreiro, J. S. Casas, M. D. Couce, A. Sánchez, A. Sánchez-Gonzalez, J. Sordo, and E.
437 M. Vázquez-López, *J. Inorg. Biochem.*, 138 (2014) 89-98.
- 438 [62] E. Barreiro, J. S. Casas, M. D. Couce, A. Sánchez, J. Sordo, E. M. Vázquez-López, J
439 *Inorg Biochem.* 131 (2014) 68–75.
- 440 [63] R. Kivekäs, E. Colacio, J. Ruiz, J. D. López-González, P. León, *Inorg Chim Acta.* 159
441 (1989)103–110.
- 442 [64] L. Ortego, F. Cardoso, S. Martins, M. F. Fillat, A. Laguna, M. Meireles, M. D.
443 Villacampa, M. C. Gimeno, *J Inorg Biochem.* 130 (2014) 32–37.
- 444 [65] I. Ott, T. Koch, H. Shorafa, Z. Bai, D. Poeckel, D. Steinhilber, R. Gust, *Org Biomol*
445 *Chem.* 3 (2005) 2282–2286.
- 446 [66] Agilent, Crys Alis PRO. Agilent Technologies Yarnton England. (2011).
- 447 [67] G.M. Sheldrick, *Acta Cryst. A*64 (2008) 112–122.
- 448 [68] SCALE3 ABSPACK An Oxford Diffraction program. (1.0.4, gui:1.0.3) (C) Oxford
449 Diffraction Ltd. (2005).
- 450 [69] C.F. Macrae, P.R. Edgington, P. McCabe, E. Pidcock, G.P. Shields, R. Taylor,
451 M. Towler, J. van de Streek, *J Appl Cryst.* 39 (2006) 453–457.
- 452 [70] M.B. Hansen, S.E. Nielsen, K. Berg, *J Immunol Methods.* 119 (1989) 203–210.
- 453

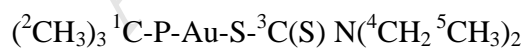
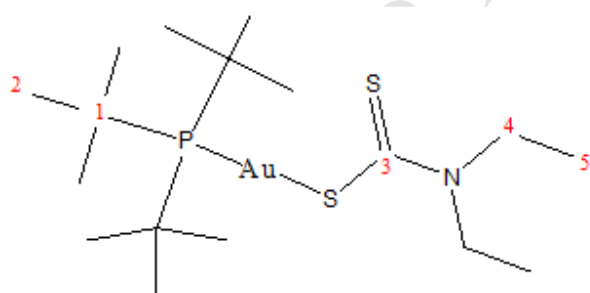
Complex (1)



Complex (2)



Complex (3)



Scheme 1: Skeletal structures and condensed formulae of complexes (1), (2) and (3)

representing non-equivalent carbons and protons for ^{13}C and ^1H NMR data.

Table 1: IR frequencies (cm⁻¹) of free ligands and complexes (2) and (3)

	Stretch	Bend	Stretch	Bend	Stretch	Stretch
Free ligand/complex	C-H(CH ₃)	C-H(CH ₃)	C-H(CH ₂)	C-H(CH ₂)	C=S	S=C-N
Free dimethyl dithiocarbamate	2924	1360	----	-----	962	1488
(2)	962(asym), 2869 (sym)	1372	----	-----	1022, 972	1479
Free diethyl dithiocarbamate	2925	1358	2979	1379	986	1466
(3)	2965(asym), 2867 (sym)	1371	2925	1409	1020, 989	1478

Table 2: Solution ¹H NMR chemical shifts (ppm) of the free gold(I) metal precursor 1 and complexes 2 and 3.

Free ligand/complex	2-H	4-H	5-H
(1)	1.52	-	-
Free NaS ₂ CN(CH ₃) ₂ ·H ₂ O	-	3.55	-
(2)	1.55	3.48	-
Free NaS ₂ CN(C ₂ H ₅) ₂ ·3H ₂ O	-	1.23	4.03
(3)	1.53	1.31	3.92

Table 3: Solution ^{13}C and ^{31}P NMR chemical shifts (ppm) of the free gold(I) metal precursor (1) and Au(I) complexes (2) and (3)

Free ligand/complex	C=S	C-1 (J_{PC} in Hz)	C-2	C-4	C-5	^{31}P
(1)	-	39.42(20.6)	32.23	-	-	200.02
Free $\text{NaS}_2\text{CN}(\text{CH}_3)_2 \cdot \text{H}_2\text{O}$	212.82	-	-	45.12	-	-
(2)	207.49	39.31(17.5)	32.21	45.16	-	207.49
Free $\text{NaS}_2\text{CN}(\text{C}_2\text{H}_5)_2 \cdot 3\text{H}_2\text{O}$	206.7	-	-	49.61	12.31	
(3)	205.92	39.39(17.5)	32.24	49.03	12.21	205.87

Table 4: IC_{50} Values (μM) of gold(I) complexes against A549, MCF7 and , HeLa cancer cell lines.

Complex	A549	MCF7	HeLa
Cisplatin	41.60 ± 3.00	22.38 ± 0.62	19.40 ± 1.85
(1)	14.30 ± 0.81	16.71 ± 0.80	16.03 ± 1.01
(2)	26.90 ± 1.04	21.07 ± 0.95	2.11 ± 0.43
(3)	19.40 ± 0.64	16.00 ± 0.83	3.18 ± 0.54

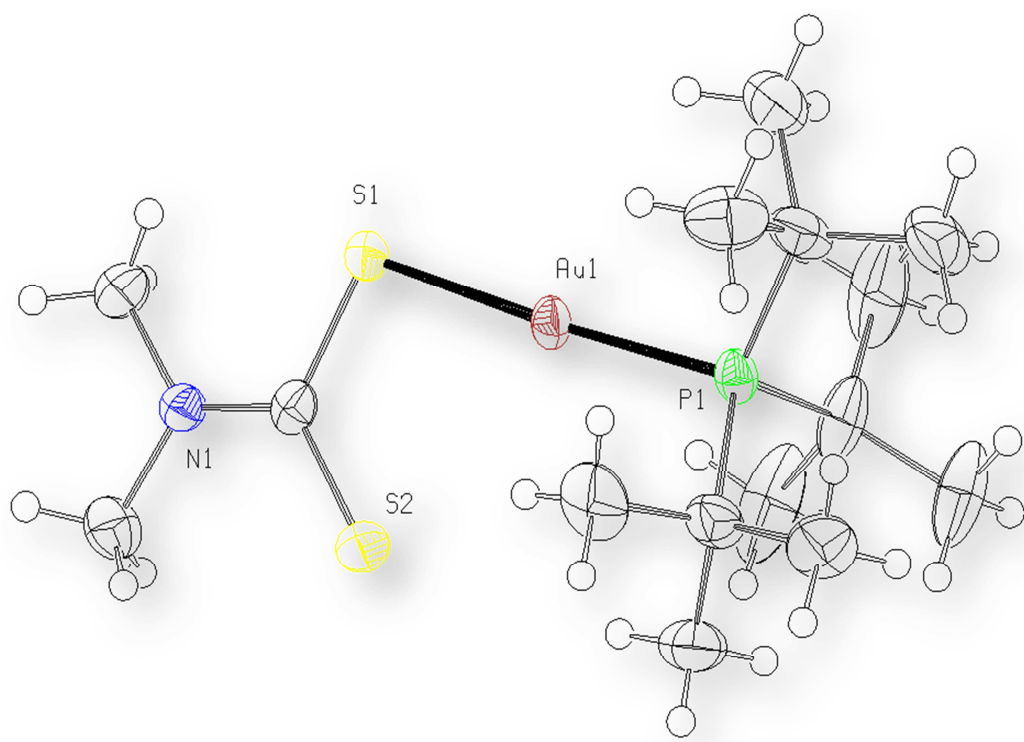
Table 5 : Crystallographic characteristics, experimental and structure refinement details for crystal structure of complexes (2) and (3)

	Complex (2)	Complex (3)
Empirical formula	C ₁₅ H ₃₃ AuNPS ₂	C ₁₇ H ₃₇ AuNPS ₂
Empirical formula weight	519.48	547.53
Crystal size/mm	0.2 × 0.2 × 0.05	0.1 × 0.1 × 0.1
Wavelength/Å	0.71073	0.71073
Temperature/K	200	200
Crystal symmetry	Monoclinic	Orthorhombic
Space group	P 21/c	P 21 21 21
a/Å	14.3661 (9)	13.6063 (8)
b/Å	12.5419 (6)	13.6398 (9)
c/Å	11.6216 (7)	23.7965 (13)
β/°	103.910 (6)	90
V/ Å ³	2032.6 (2)	4416.3 (5)
Z	4	8
Dc/Mg m ⁻³	1.698	1.647
μ(Mo-Kα)/mm ⁻¹	7.515	6.922
F(000)	1024	2176
θ Limits/°	3.1–29.0	3.0–29.1
Collected reflections	10518	37465
Unique reflections(R _{int})	4774 (0.043)	9929 (0.043)
Observed reflections [F _o > 2σ(F _o)]	3391	10949
Goodness of fit on F ²	1.03	1.05
R ₁ (F), ^a [I > 2σ(I)]	0.037	0.035
wR ₂ (F ²), ^b [I > 2σ(I)]	0.095	0.082

Largest diff. peak, hole/e Å ⁻³	0.93, -1.78	3.26, -0.73
Flack (Absolute structure parameter)	-	-0.008 (6)

Table 6: Selected bond angles (°) and bond lengths (Å) for complexes (2) and (3)

Bond Lengths (Å)		Bond Angles (°)	
Complex (2)			
Au1—P1	2.2743 (14)	P1—Au1—S1	176.44 (4)
Au1—S1	2.3247 (15)	C1—S1—Au1	99.66 (17)
Complex (3)			
Au1—P1	2.2818 (15)	P1—Au1—S1	172.74 (6)
Au1—S1	2.3293 (15)	C1—S1—Au1	101.7 (2)
Au2—P2	2.2753 (16)		
Au2—S3	2.3139 (16)		



521

522 Figure 1: A view of the molecular structure of mononuclear complex (2), with partial atom
523 labelling scheme and displacement ellipsoids drawn at 50% probability level.

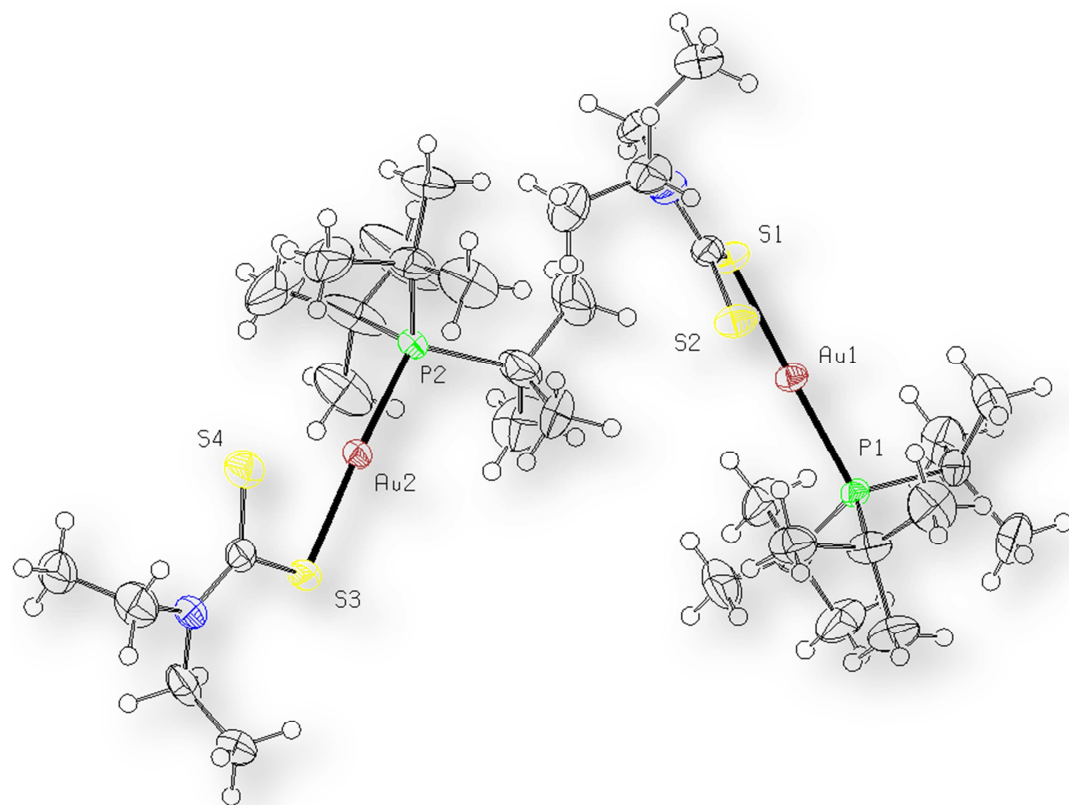


Figure 2: A view of the molecular structure of mononuclear complex (**3**), with partial atom labelling scheme and displacement ellipsoids drawn at 50% probability level.

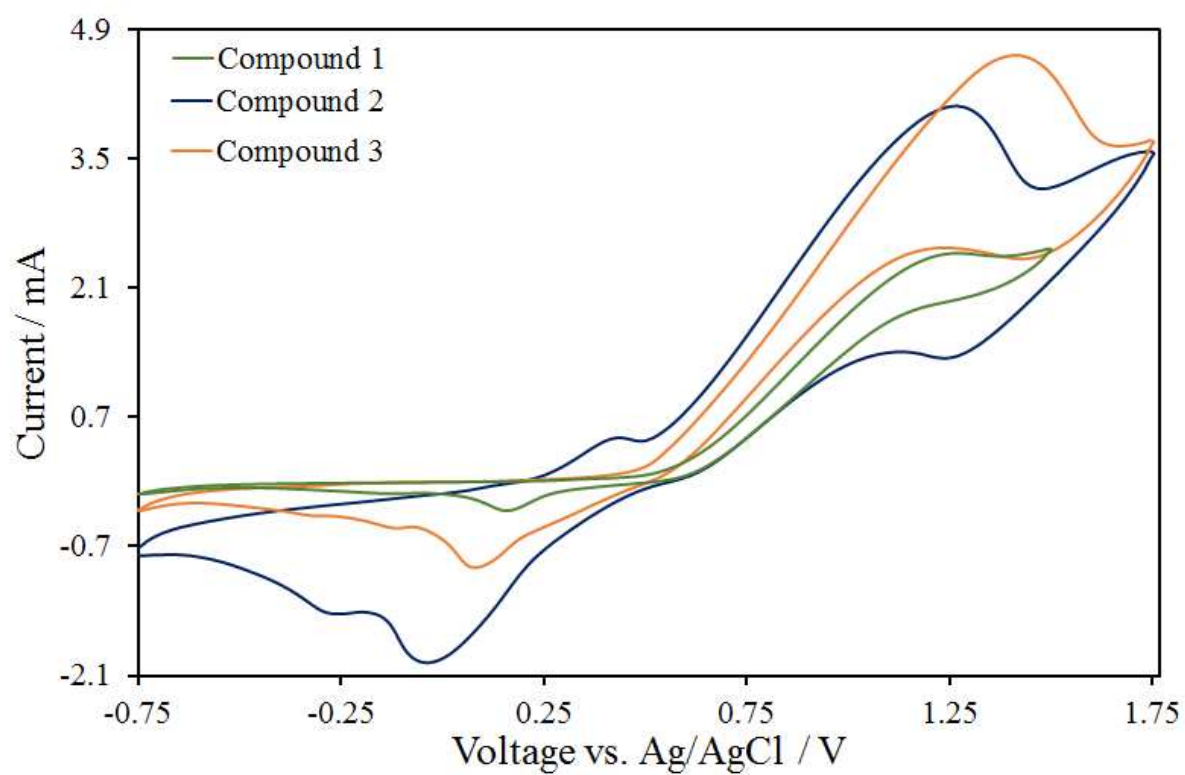


Figure 3 Cyclic voltammograms of complexes (**1**, **2** and **3**) at platinum electrode.

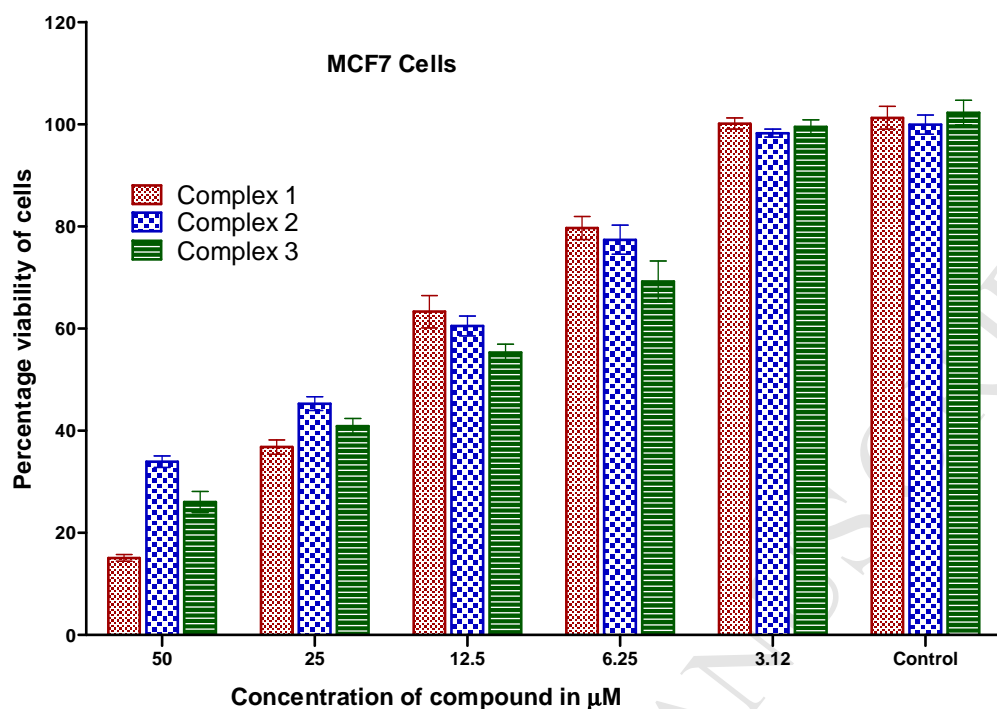


Figure 4: Graph showing the cytotoxic effect of series of concentrations of compounds (1-3) on viability of MCF 7 cells.

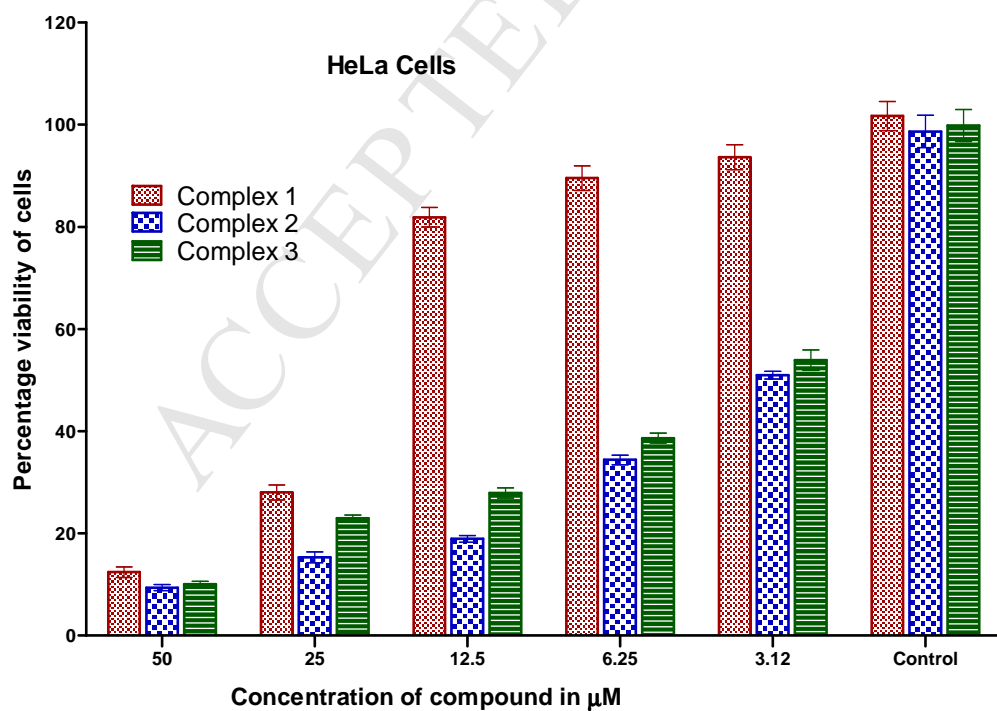


Figure 5: Graph showing the cytotoxic effect of series of concentrations of compounds (**1-3**) on viability of HeLa cells.

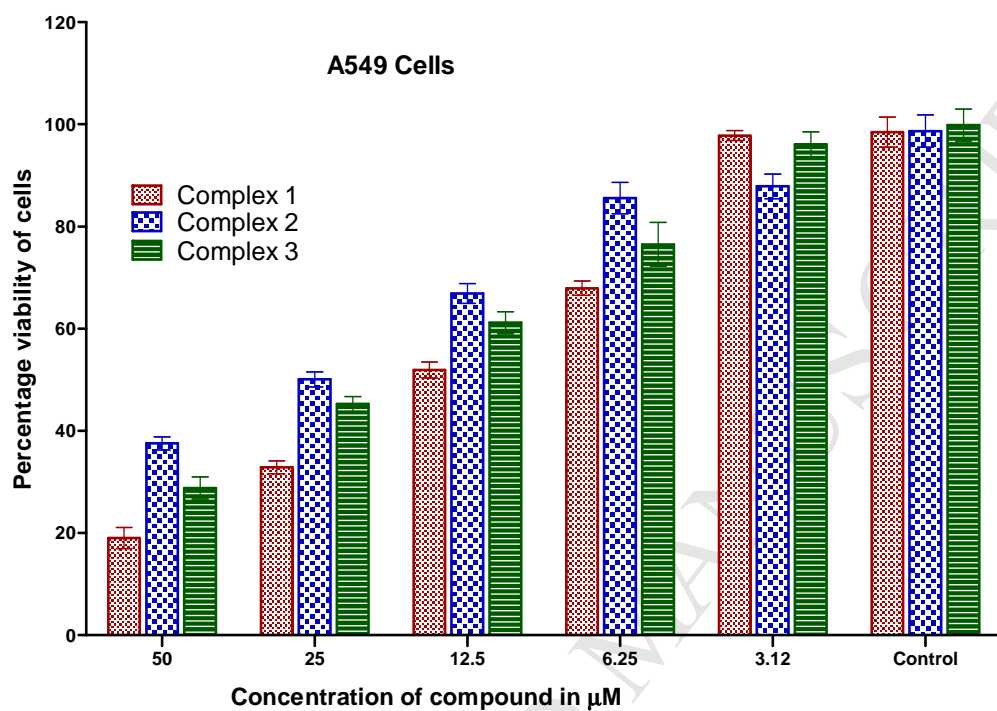


Figure 6: Graph showing the cytotoxic effect of series of concentrations of compounds (**1-3**) on viability of A549 cells.

- Gold(I) complexes of the type P-Au(I)-S were synthesized.
- Cytotoxicity of complexes measured on A549, HeLa and MCF7 cell lines.
- X-ray data shows the gold coordination sphere adopts a linear geometry

Following Figures and a Table can be utilized as supplementary materials:

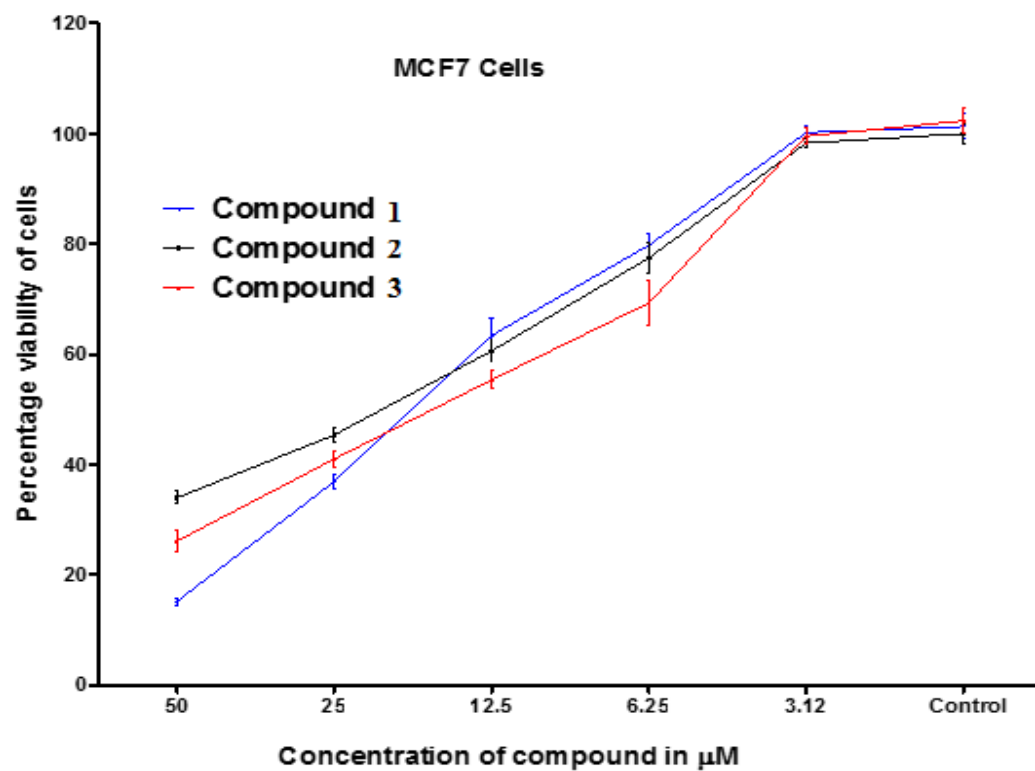


Figure S1 Concentration dependent *in vitro* cytotoxic effects of compounds (1-3) on MCF7 cells.

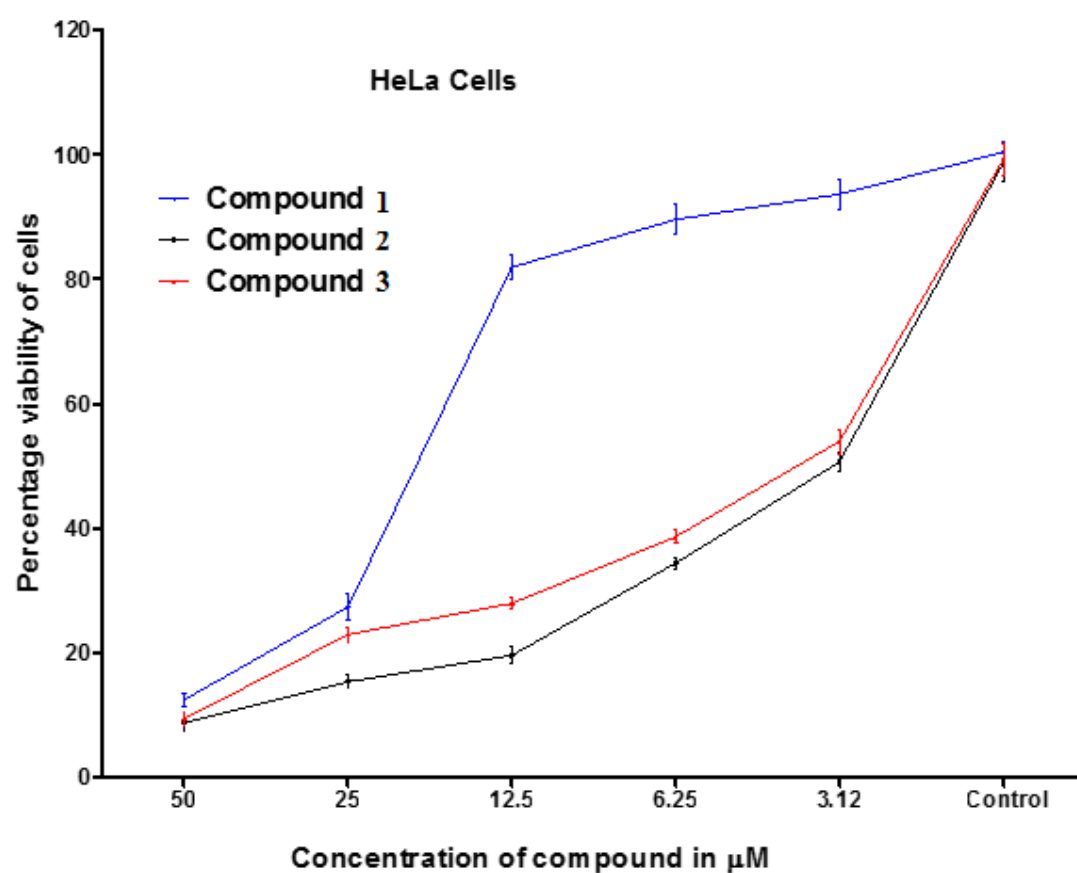


Figure S2 Concentration dependent *in vitro* cytotoxic effects of compounds (1-3) on HeLa cells.

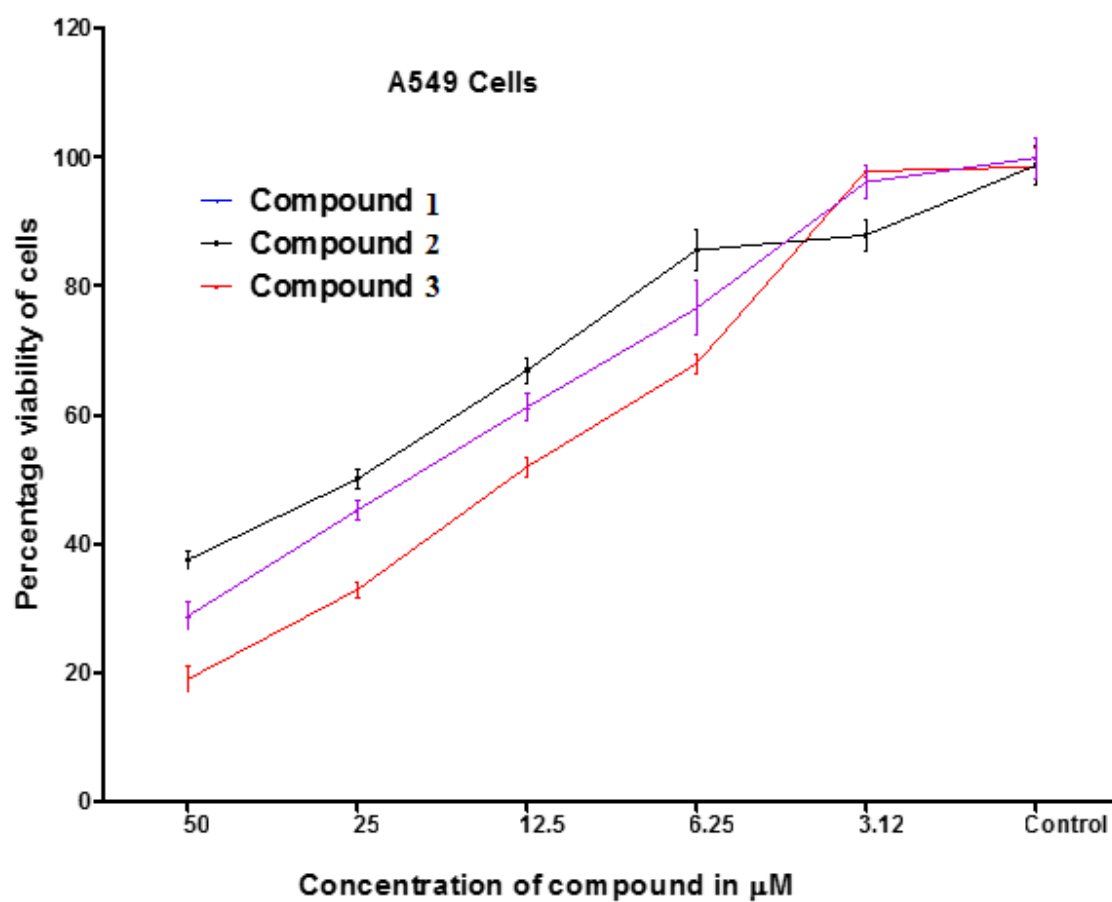


Figure S3 Concentration dependent *in vitro* cytotoxic effects of compounds (1-3) on A549 cells.

Table 1: *in vitro* cytotoxic effect of series of concentrations (μM) of gold(I) complexes on percent viability of HeLa (human cervical cancer)

μM	Complex (1)	Complex (2)	Complex (3)
Control	100.9 ± 2.9	98.7 ± 2.7	99.8 ± 2.4
3.12	93.6 ± 2.4	50.6 ± 1.5	53.9 ± 1.9
6.25	89.5 ± 2.3	34.4 ± 0.9	38.6 ± 1.2
12.5	81.9 ± 1.9	19.5 ± 1.4	27.9 ± 1.0
25	27.3 ± 1.5	15.3 ± 1.1	22.9 ± 1.2
50	12.4 ± 1.1	8.7 ± 1.2	9.41 ± 1.16

Supplementary material

Synthesis, characterization and anticancer activity of gold(I) complexes that contain tri-tert-butylphosphine and dialkyl dithiocarbamate ligands

Muhammad Altaf^{h*}, M. Monim-ul-Mehboob^a, Adam A. A. Seliman^a, Manzar Sohail^b, Mohammed I. M. Wazeer^a, Anvarhusein A. Isab^a, L. Li^c, V. Dhuna^d, G. Bhatia^c, K. Dhuna^e

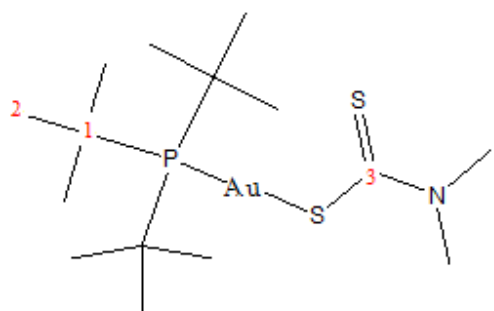
^aDepartment of Chemistry, King Fahd University of Petroleum and Minerals, Dhahran 31261, Saudi Arabia

^bCenter of Excellence in Nanotechnology, King Fahd University of Petroleum and Minerals, Dhahran 31261, Saudi Arabia

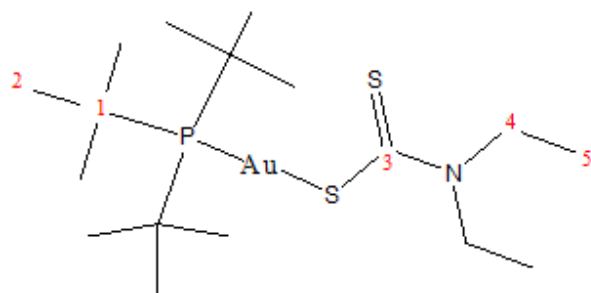
^cKing Abdullah University of Science and Technology (KAUST), Thuwal 23955-6900, Jeddah, Saudi Arabia

^dDept. of Molecular Biology and Biochemistry, Guru Nanak Dev University, Amritsar-143005, Punjab, India

^eDepartment of Molecular Biology and Biochemistry, Guru Nanak Dev University, Amritsar – 143005, Punjab, India



[t-Bul₃PAuS₂CN(CH₃)₂] (1)



[t-Bu₃PAuS₂CN(CH₃)₂] (**2**)

Scheme S1: Skeletal structures and condensed formulae of compounds **0**, **1** and **2**

representing non-equivalent carbons and protons for ¹³C and ¹H NMR data.

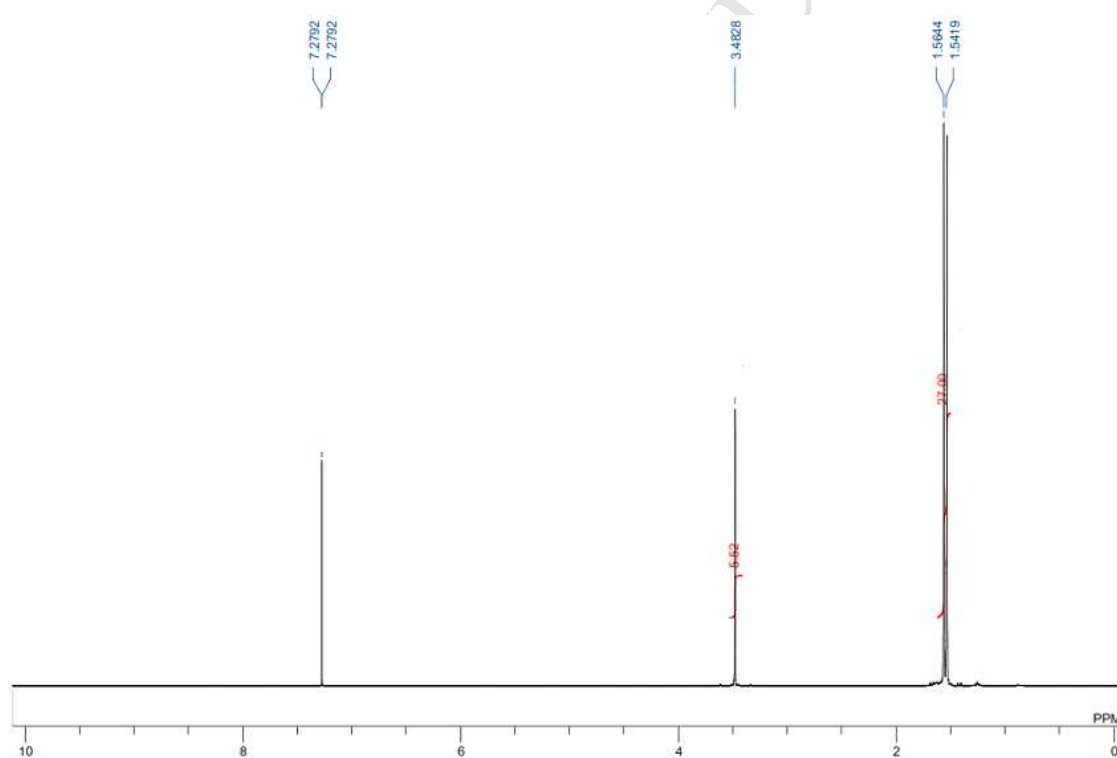


Figure S1: ¹H NMR spectrum of compound **2**.

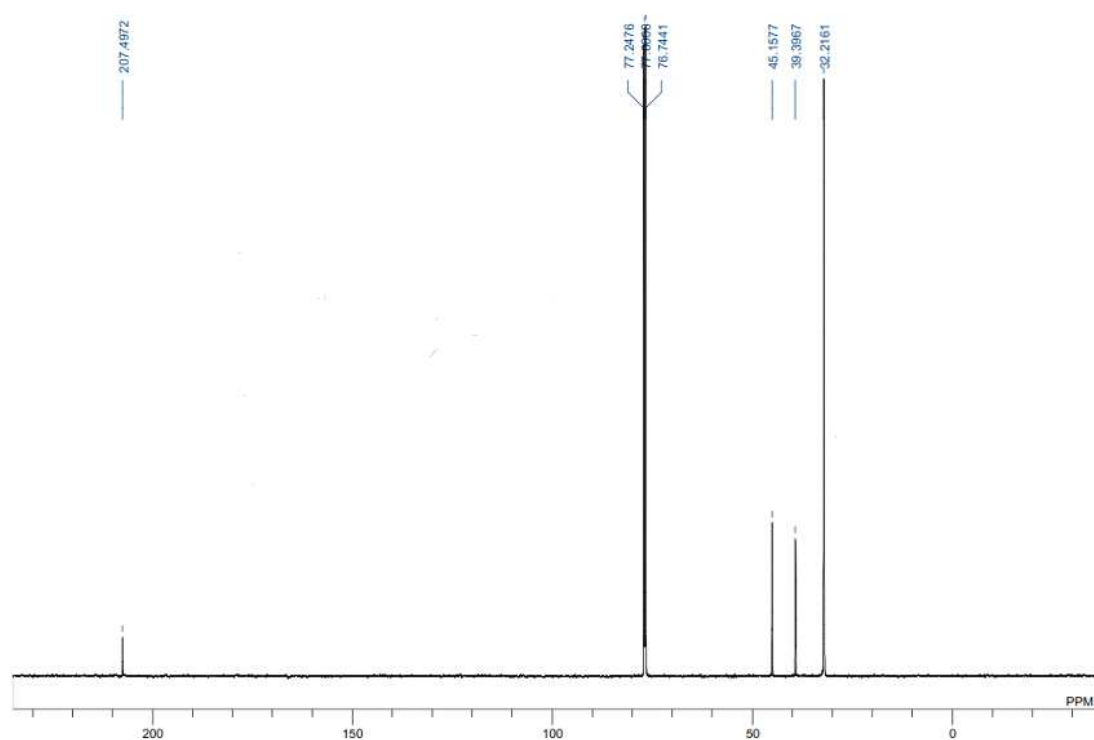


Figure S2: ¹³C NMR spectrum of compound 2.

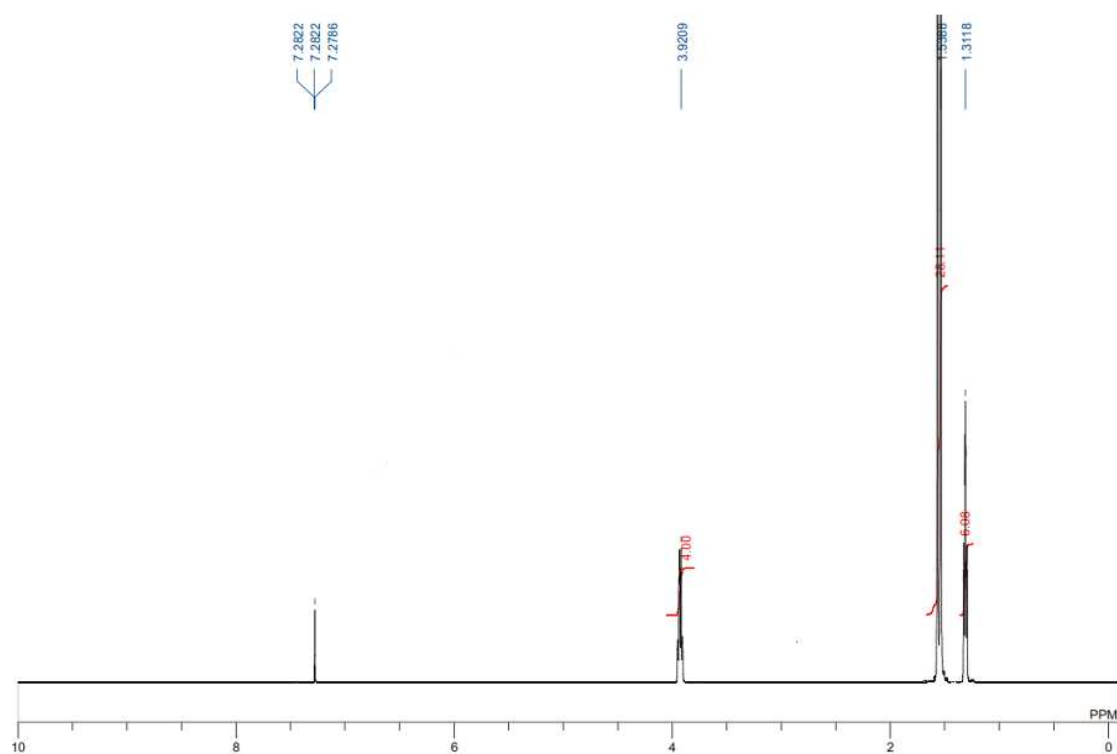


Figure S3: ¹H NMR spectrum of compound **3**.

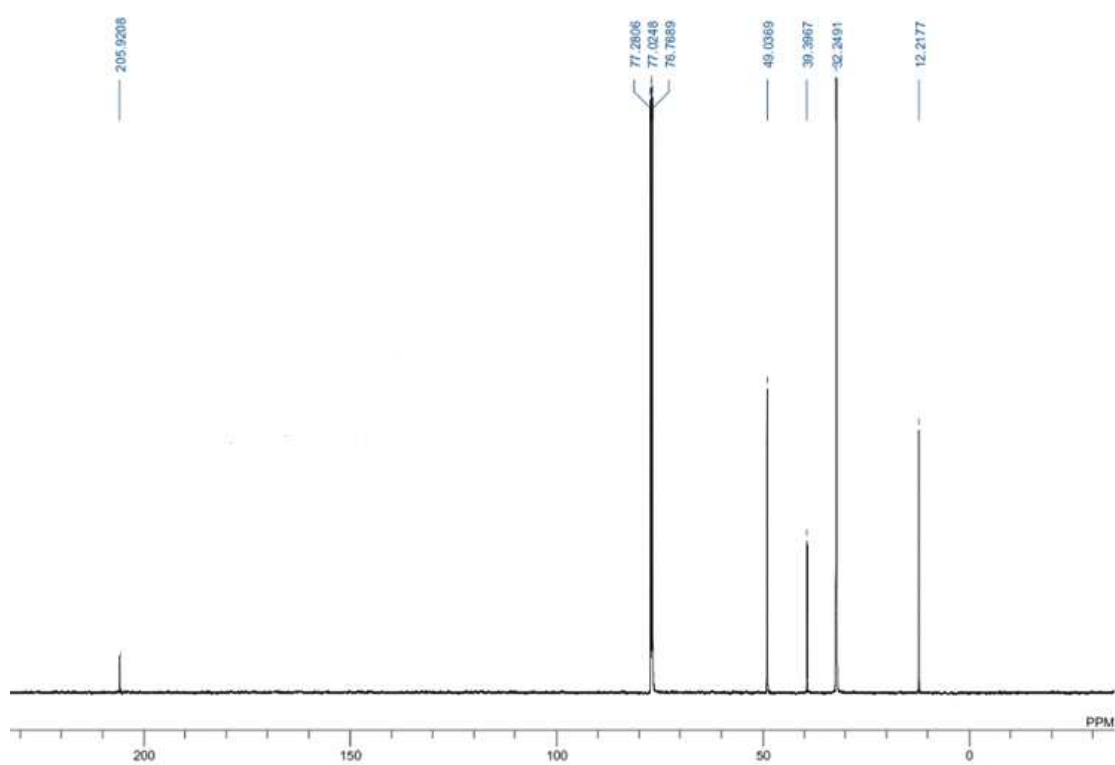


Figure S4: ¹³C NMR spectrum of compound 3.